07.2

Deep ultraviolet photodetectors based on the $In_2O_3-Ga_2O_3$ mixed compounds films

© D.A. Almaev[1], A.V. Almaev[1,2], V.I. Nikolaev[3,4], P.N. Butenko[1,3], M.P. Scheglov[3], A.V. Chikiryaka[3], A.I. Pechnikov[3]

[1] Tomsk State University, Tomsk, Russia
[2] Fokon LLC, Kaluga, Russia
[3] Ioffe Institute, St. Petersburg, Russia
[4] Perfect Crystals LLC, Saint-Petersburg, Russia
E-mail: almaev001@mail.ru

Received October 9, 2023
Revised November 22, 2023
Accepted November 22, 2023

The photoelectrical characteristics of the $In_2O_3-Ga_2O_3$ mixed compounds films grown by halide vapor-phase epitaxy on sapphire substrates were studied. The studied films were a mixture of cubic δ-Ga_2O_3 and c-In_2O_3 phases. The obtained results for $In_2O_3-Ga_2O_3$ mixed compounds, $\varepsilon(\kappa)$-Ga_2O_3 and c-In_2O_3 films grown at similar conditions were compared. The $In_2O_3-Ga_2O_3$ mixed compounds films demonstrated the highest photosensitivity, operation rate and a low base resistance. The quantum efficiency was $6.9 \cdot 10^3$% at an electric-field strength of 1 kV/cm, which was significantly higher than in the known literature. It is assumed, that the high photosensitivity was caused by the generation of charge carriers in the δ-Ga_2O_3 regions formed between c-In_2O_3 with a high electron concentration.

Keywords: Gallium oxide, indium oxide, UV photodetector, halide vapor phase epitaxy, photoelectrical characteristics.

DOI: 10.61011/PJTF.2024.05.57176.19759

Solar-blind ultraviolet (UV) photodetectors have been studied extensively in recent years, since their potential applications include (but are not limited to) wireless telecommunications, flame detection, ozone hole monitoring, and chemical and biological analysis [1,2]. Current studies are focused on wide-gap oxide and nitride semiconductors. It appears that Ga_2O_3 is the most promising among them, since the intrinsic absorption edge of this compound is within the solar-blind region. The process of growth of Ga_2O_3 crystals of a high structural quality is less complex and costly than the production of most wide-gap semiconductors [1–6].

There is no doubt that Ga_2O_3 attracts much research interest and has bright prospects for application in photoelectronics. The photovoltaic properties of In_2O_3 are poorly studied, but a combination of these semiconductors in a composite may open up new applications for current Ga_2O_3-based photodetectors. Solid solutions and composites based on indium gallium oxide (IGO) are used widely in power electronics, gas sensorics, and photonics [7–13]. IGO is used to fabricate Schottky barrier diodes and thin-film transistors [7,8]. In the present study, we report the results of examination of photoelectrical characteristics (PECs) of gallium and indium oxides and a mixed compound based on them.

Films of c-In_2O_3, $\varepsilon(\kappa)$-Ga_2O_3, and IGO were fabricated by halide vapor phase epitaxy (HVPE) with gaseous $InCl_3$, GaCl, and O_2 used as precursors. These c-In_2O_3, $\varepsilon(\kappa)$-Ga_2O_3, and IGO films were grown on the c-plane of sapphire substrates 430 μm in thickness at a temperature of 600, 500, and 625°C, respectively. The thickness of grown films was determined to be 500 nm by examining images of their cleaved faces. Notably, this thickness varied within 3% over the wafer. No intentional doping of films was performed in the process of growth. Prior to epitaxial growth of a $\varepsilon(\kappa)$-Ga_2O_3 layer, a buffer α-Ga_2O_3 layer was deposited onto the sapphire substrate surface. Platinum contacts were deposited onto the surfaces of films by magnetron sputtering through a mask in order to examine their electrophysical properties. The interelectrode distance was 150 μm for c-In_2O_3 and IGO and 1 mm for $\varepsilon(\kappa)$-Ga_2O_3. A Nextron microprobe setup and a Keithley 2636A sourcemeter were used in PEC studies. PECs were determined at room temperature without illumination and under illumination by radiation with wavelength $\lambda = 254$ nm. A krypton–fluorine lamp with radiation flux density $P = 1.3$ mW/cm^2 served as a source of monochromatic radiation.

The procedure and results of structural studies were discussed in detail in [14]. The results of X-ray diffraction (XRD) analysis of Ga_2O_3 films revealed peaks from $\varepsilon(\kappa)$-Ga_2O_3 and α-Ga_2O_3. The XRD pattern of In_2O_3 featured c-In_2O_3 peaks corresponding to reflections from planes (222) and (004). A multitude of peaks associated with c-In_2O_3 and δ-Ga_2O_3 were observed in the XRD spectrum of IGO. The comparison of PECs of $\varepsilon(\kappa)$-Ga_2O_3 films and films of IGO, which has δ-Ga_2O_3 in its composition, is valid, since they were fabricated in similar conditions.

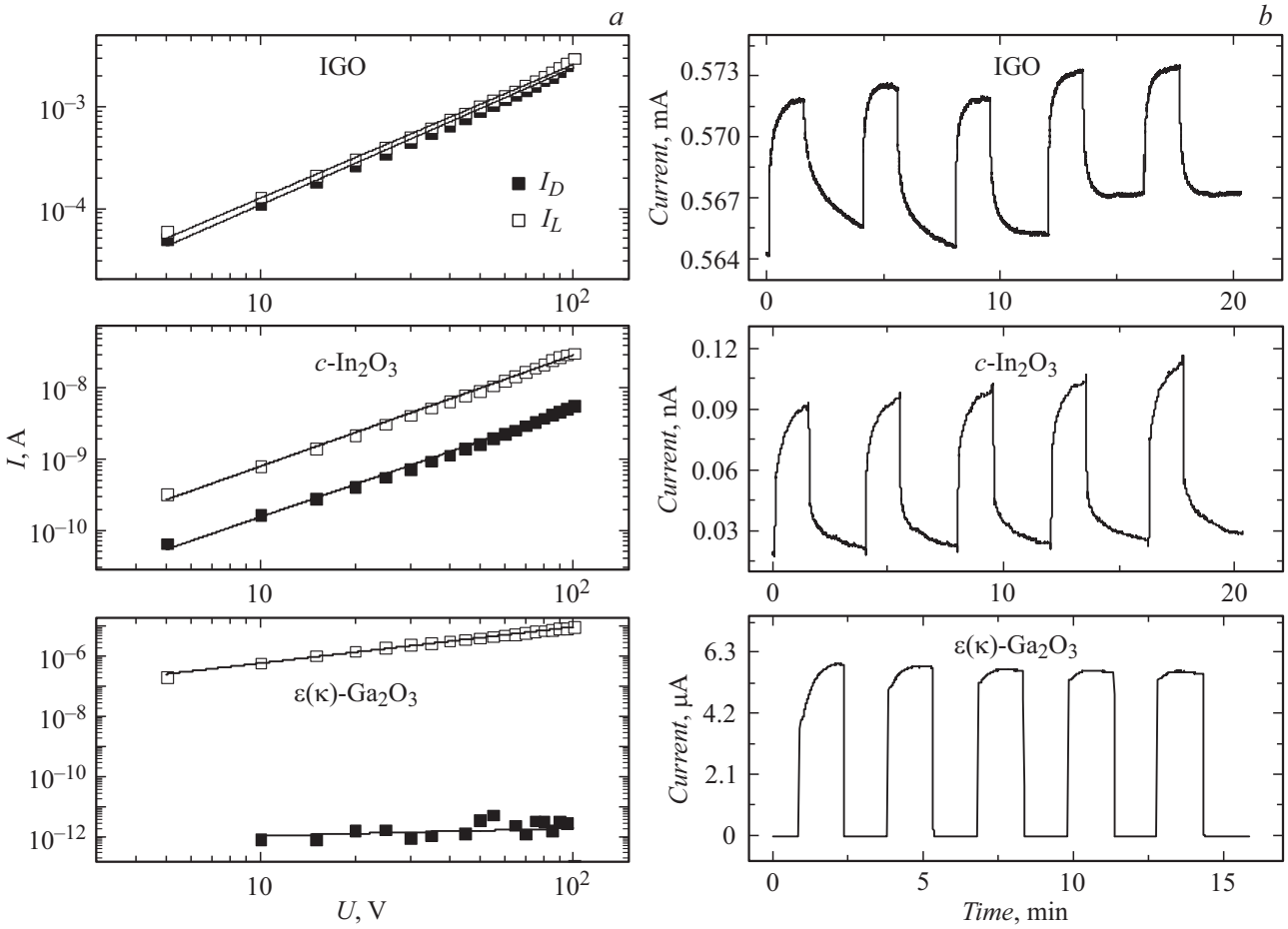

$I-V$ characteristics(a) and time dependences of current (b) for IGO, c-In_2O_3, and $\varepsilon(\kappa)$-Ga_2O_3 films without and with illumination by radiation with $\lambda = 254$ nm and $P = 1.3$ mW/cm^2.

According to the energy-dispersive X-ray spectroscopy data, the ratio of concentrations of In and Ga atoms is 5.5:1.1. This indicates that c-In_2O_3 dominates over δ-Ga_2O_3 in IGO films.

The current.voltage ($I-V$) characteristics of IGO, c-In_2O_3, and $\varepsilon(\kappa)$-Ga_2O_3 films (see the left panel of the figure) are symmetric and reveal a power-law dependence: $I \propto U^m$, where m is the index of power. The values of m for dark current (I_D) and current under illumination (I_L) are almost matching within the measurement accuracy. These values for IGO, c-In_2O_3, and $\varepsilon(\kappa)$-Ga_2O_3 were 1.31 ± 0.01, 1.52 ± 0.02, and 1.21 ± 0.02, respectively. The values of I_L for c-In_2O_3 and IGO films tend to saturation when $U = 95$ and 80 V is reached, respectively. This effect was not observed in $\varepsilon(\kappa)$-Ga_2O_3 films at voltages up to $U = 200$ V, since these samples are less conductive and have a greater distance between contacts. The rate of response of photodetectors based on IGO, c-In_2O_3, and $\varepsilon(\kappa)$-Ga_2O_3 may be evaluated by examining the time dependences of current under cyclic illumination (see the right panel of the figure). The photoconductivity rise and fall times were 8.4 ± 0.1 and 14.7 ± 0.1 s for IGO, 14.3 ± 0.2 and 25.0 ± 0.4 s for c-In_2O_3, and 23.7 ± 0.1 and 5.1 ± 0.1 s for $\varepsilon(\kappa)$-Ga_2O_3, respectively. Insignificant variations of I_D and I_L with time were observed for c-In_2O_3 and IGO films. According to [12,15], this may be related to the ionization of oxygen vacancies (V_O) and surface states of films induced by O_2 desorption under the influence of UV radiation. The relatively low rate of response of $\varepsilon(\kappa)$-Ga_2O_3 films is attributable to the well-known effect of residual photoconductivity of Ga_2O_3 [16].

The key PECs determined from $I-V$ characteristics in accordance with the formulae given in [1,2] at electric-field strength $E = 1$ kV/cm are listed in the table. The photosensitivity of c-In_2O_3 films is the lowest. The responsivity (R^*), the calculated quantum efficiency (η'), and the photocurrent (I_{ph}) are considered to be the most important parameters for a photodetector. All of them are governed by I_L. It then turns out that IGO is the optimum material among all the examined ones. In real-world conditions, the detectivity (D^*) and the ratio of I_{ph} to I_D (PDCR) may be no less important for a photodetector, since they specify the minimum detectable signal intensity and the signal-to-noise ratio, respectively. The values of D^* and PDCR, which are affected by I_D, for IGO are substantially lower than the corresponding values for $\varepsilon(\kappa)$-Ga_2O_3.

When the studied samples were irradiated with UV light, non-equilibrium electrons and holes were produced in their

PECs of IGO, c-In_2O_3 and $\varepsilon(\kappa)$-Ga_2O_3 films at $E = 1\,\text{kV/cm}$, $\lambda = 254\,\text{nm}$, and $P = 1.3\,\text{mW/cm}^2$

Material	I_{ph}, A	PDCR, a. u.	R^*, A/W	D^*, cm · $\text{Hz}^{0.5}$/W	η', %
IGO	$2.9 \cdot 10^{-5}$	0.2	14.2	$7.2 \cdot 10^{10}$	$6.9 \cdot 10^3$
c-In_2O_3	$1.2 \cdot 10^{-9}$	4.3	$6.2 \cdot 10^{-4}$	$2.5 \cdot 10^9$	0.3
$\varepsilon(\kappa)$-Ga_2O_3	$9.9 \cdot 10^{-6}$	$7.1 \cdot 10^6$	0.8	$1.1 \cdot 10^{14}$	373.4

bulk. These carriers get separated under the influence of an external electric field and drift toward contacts. The calculated carrier collection efficiency is characterized by the value of η', which is defined as the product of theoretical quantum efficiency η and photoresistor gain Γ. If we assume that $\eta = 100\%$, $\eta' = \Gamma$. This corresponds to the ratio between the lifetime of carriers and the time of their drift between contacts [17]. The value of η' is then specified by the concentration of V_O and other structural defects that have the capacity to capture a hole. Owing to the presence of a buffer layer and the use of an epitaxial growth technique, $\varepsilon(\kappa)$-Ga_2O_3 is likely to feature a low density of structural defects. This is verified by low values of I_D and is reflected in the values of η' that are fairly modest for Ga_2O_3 . Presumably, the high photosensitivity of IGO at $\lambda = 254\,\text{nm}$ rests on bipolar generation of carriers in formed cubic δ-Ga_2O_3 regions in the c-In_2O_3 matrix. In addition, the formation of IGO is accompanied by high defect levels [14]; this is the reason why the values of η' turned out to be an order of magnitude higher than those for $\varepsilon(\kappa)$-Ga_2O_3 and exceeded considerably the values reported in literature [10–13].

Thus, the photoelectrical characteristics of IGO films grown by HVPE were examined and compared to the corresponding parameters of $\varepsilon(\kappa)$-Ga_2O_3 and c-In_2O_3 films fabricated in similar conditions. IGO films featured the highest photosensitivity and rate of response. The values of photocurrent and calculated quantum efficiency at $E = 1\,\text{kV/cm}$ were $2.9 \cdot 10^{-5}\,\text{A}$ and $6.9 \cdot 10^3\%$, respectively, and exceeded considerably the values reported in literature. The photoconductivity rise and fall times for IGO films at $U = 2\,\text{V}$ were 8.4 and 14.7 s, respectively. A mechanism explaining the high photosensitivity of IGO was proposed.

Funding

This study was supported financially by the Russian Science Foundation (grant No. 20-79-10043 P).

Conflict of interest

The authors declare that they have no conflict of interest.

References

[1] X. Hou, Y. Zou, M. Ding, Y. Qin, Z. Zhang, X. Ma, P. Tan, S. Yu, X. Zhou, X. Zhao, G. Xu, H. Sun, S. Long, J. Phys. D: Appl. Phys., **54** (4), 043001 (2020). DOI: 10.1088/1361-6463/abbb45

[2] D. Kaur, M. Kumar, Adv. Opt. Mater., **9** (9), 2002160 (2021). DOI: 10.1002/adom.202002160

[3] J. Moloney, O. Tesh, M. Singh, J.W. Roberts, J.C. Jarman, L.C. Lee, T.N. Huq, J. Brister, S. Karboyan, M. Kuball, P.R. Chalker, R.A. Oliver, F.C.-P. Massabuau, J. Phys. D: Appl. Phys., **52** (47), 475101 (2019). DOI: 10.1088/1361-6463/ab3b76

[4] X.Y. Sun, X.H. Chen, J.G. Hao, Z.P. Wang, Y. Xu, H.H. Gong, Y.J. Zhang, X.X. Yu, C.D. Zhang, F.-F. Ren, S.L. Gu, R. Zhang, J.D. Ye, Appl. Phys. Lett., **119** (14), 141601 (2021). DOI: 10.1063/5.0059061

[5] D.A. Almaev, A.V. Almaev, V.V. Kopyev, V.I. Nikolaev, A.I. Pechnikov, S.I. Stepanov, M.E. Boyko, P.N. Butenko, M.P. Scheglov, Tech. Phys. Lett., **48** (11), 61 (2022). DOI: 10.21883/TPL.2022.11.54893.19322.

[6] V.M. Kalygina, O.S. Kiselyeva, B.O. Kushnarev, V.L. Oleinik, Yu.S. Petrova, A.V. Tsymbalov, Semiconductors, **56** (9), 707 (2022). DOI: 10.21883/SC.2022.09.54139.9868.

[7] H. Wenckstern, D. Splith, A. Werner, S. Müller, M. Lorenz, M. Grundmann, ACS Comb. Sci., **17** (12), 710 (2015). DOI: 10.1021/acscombsci.5b00084

[8] Y.-C. Cheng, S.-P. Chang, C.-P. Yang, S.-J. Chang, Appl. Phys. Lett., **114** (19), 192102 (2019). DOI: 10.1063/1.5086457

[9] E. Lopez-Aymerich, G. Domenech-Gil, M. Moreno, P. Pellegrino, A. Romano-Rodriguez, Sensors, **21** (10), 3342 (2021). DOI: 10.3390/s21103342

[10] Z. Zhang, H. Wenckstern, J. Lenzner, M. Lorenz, M. Grundmann, Appl. Phys. Lett., **108** (12), 123503 (2016). DOI: 10.1063/1.4944860

[11] U.U. Muazzam, M.S. Raghavan, A.S. Pratiyush, R. Muralidharan, S. Raghavan, D.N. Nath, S.A. Shivashankar, J. Alloys Compd., **828**, 154337 (2020). DOI: 10.1016/j.jallcom.2020.154337

[12] F. Zhang, H. Li, M. Arita, Q. Guo, Opt. Mater. Express, **7** (10), 3769 (2017). DOI: 10.1364/OME.7.003769

[13] S.-P. Chang, L.-Y. Chang, J.-Y. Li, Sensors, **16** (12), 2145 (2016). DOI: 10.3390/s16122145

[14] N.N. Yakovlev, A.V. Almaev, V.I. Nikolaev, B.O. Kushnarev, A.I. Pechnikov, S.I. Stepanov, A.V. Chikiryaka, R.B. Timashov, M.P. Scheglov, P.N. Butenko, D.A. Almaev, E.V. Chernikov, Mater. Today Commun., **34**, 105241 (2023). DOI: 10.1016/j.mtcomm.2022.105241

[15] D. Shao, L. Qin, S. Sawyer, IEEE Photon. J., **4** (3), 715 (2012). DOI: 10.1109/JPHOT.2012.2195485

[16] K. Arora, N. Goel, M. Kumar, M. Kumar, ACS Photon., **5** (6), 2391 (2018). DOI: 10.1021/acsphotonics.8b00174

[17] A.V. Voitsekhovskii, I.I. Inzhin, V.P. Savchin, N.M. Vakiv, *Fizicheskie osnovy poluprovodnikovoi fotoelektroniki* (Izd. Tomsk. Gos. Univ., Tomsk, 2013), pp. 349–353 (in Russian).

Translated by D.Safin